Published in final edited form as:
Mol Immunol. 2009 February ; 46(5): 793–802. doi:10.1016/j.molimm.2008.09.002.

Endosomal Trafficking of the Ligated FcεRI Receptor

Gul'nar V. Fattakhova[a,§], **Madhan Masilamani**[a,‡], **Sriram Nrayanan**[a], **Francisco Borrego**[a], **Alasdair M. Gilfillan**[b], **Dean D. Metcalfe**[b], and **John E. Coligan**[a,*]

a *Receptor Cell Biology Section, Laboratory of Immunogenetics, National Institute of Allergy and Infectious Diseases, National Institutes of Health, Rockville, MD 20852*

b *Mast Cell Biology Section, Laboratory of Allergic Diseases, National Institute of Allergy and Infectious Diseases, National Institutes of Health, Bethesda, MD 20892*

Abstract

In addition to initiating signaling cascades leading to mast cell mediator release, aggregation of the high affinity IgE receptor (FcεRI) leads to rapid internalization of the cross-linked receptor. However, little is known about the trafficking of the internalized FcεRI. Here we demonstrate that in RBL-2H3 cells, aggregated FcεRI appears in the early endosomal antigen 1 ($EEA1^+$) domains of the early endosomes within 15 minutes after ligation. Minimal co-localization of FcεRI with Rab5 was observed by 30 minutes, followed by its appearance in the $Rab7^+$ late endosomes and lysosomes at later time points. During endosomal sorting, FcεRI α and γ subunits remain associated. In Syk-deficient RBL-2H3 cells, the rate of transport to lysosomes is markedly increased. Taken together, our data demonstrate time-dependent sorting of aggregated FcεRI within the endosomal-lysosomal network, and that Syk may play an essential role in regulating the trafficking and retention of FcεRI in endosomes.

Keywords

FcεRI; endosomes; co-localization; Syk

1. Introduction

The high affinity IgE receptor (FcεRI) is composed of an IgE-binding α-chain, a four transmembrane-spanning β subunit and two identical disulfide-linked γ subunits (Kraft and Kinet, 2007). The aggregation of FcεRI on mast cells initiates a biochemical cascade that results in the release of inflammatory mediators. Following ligation, the receptor is rapidly internalized by either clathrin-dependent (Wilson et al., 2004) or clathrin-independent, dynamin-dependent mechanisms (Fattakhova et al., 2006). Despite the fact that FcεRI-mediated signaling in mast cells has been extensively studied (Gilfillan and Tkaczyk, 2006; Rivera and Olivera, 2007), the intracellular trafficking of the receptor and its relation to signaling have not been systematically investigated.

*Corresponding author: Tel: +1 301-496-8247; Fax: +1 301-480-2818, E-mail address: jcoligan@niaid.nih.gov.
§*Present address*: Borstel Research Center, Parkalee 22-26, D-23845 Borstel, Germany
‡*Present address*: Mount Sinai School of Medicine, Division of Pediatric Allergy & Immunology, Department of Pediatrics, One Gustave L Levy Place, New York, NY 10029

Surface receptors are endocytosed, following the binding of ligand, by a variety of potential endocytic routes (Mayor and Pagano, 2007). Electron microscopy studies have revealed that ligated FcεRI accumulates in transferrin-positive endosomal compartments (Asai et al., 2000; Oliver et al., 2007; Xue et al., 2007), and after time, localizes to structures with properties of lysosomes (Oliver et al., 2007). In addition, studies have suggested that aggregated FcεRI is endocytosed via clathrin-coated pits (Wilson et al., 2004). Our previous study (Fattakhova et al., 2006), however, revealed that, following translocation to detergent-resistant membrane fractions (conceptually termed lipid rafts), the cross-linked FcεRI remains associated with these microdomains upon internalization. Furthermore, in contrast to the aforementioned morphological studies, our data suggested that internalization of cross-linked FcεRI does not require the AP-2/clathrin complex but is dynamin-dependent.

The generalized current view of endocytosis is that intracellular vesicular traffic of internalized surface receptors is mediated by membrane fusion between receptor-containing vesicles and endocytic compartment organelles (Zerial and McBride, 2001). Each fusion step appears to be regulated by Rab proteins and phosphoinositides, generated by the action of phosphoinositide 3-kinase (PI3K). The endocytic pathway can be dissected into distinct Rab-specific compartments: the $Rab5^+$ early endosomal compartment, early/sorting endosomes ($Rab4^+$), recycling endosomes ($Rab11^+$) and the $Rab7^+$ late endosomes. Degradation of internalized receptor complexes usually occurs in LAMP-1^+ lysosomes (Markgraf et al., 2007). After internalization from the plasma membrane, proteins first enter early endosomal antigen 1 ($EEA1^+$) early endosomes (Woodman, 2000), not all of which are $Rab5^+$ (Lakadamyali et al., 2006). Thereafter, they traffic according to their fate within the endosomal network described above.

Certain surface receptors, such as the transferrin receptor, are delivered predominantly to the $Rab4^+$, $Rab11^+$ endocytic recycling compartment from where they can recycle back to the cell surface (Maxfield and McGraw, 2004). Ligation of many other surface receptors, such as the T cell receptor (TCR), predominantly results in receptor clustering that is followed by down-regulation through endocytosis and, subsequently, proteosomal and lysosomal degradation (Geisler, 2004). Rapid degradation serves to attenuate signaling via removal of activated receptor complexes. The process of endocytosis may also serve to regulate signaling pathways required for transcriptional regulation (Kapp-Barnea et al., 2006).

In this study, we examine the endocytic trafficking of internalized ligated FcεRI using confocal microscopy. We show that aggregated FcεRI first localizes to $EEA1^+$ early endosomes, and minimally co-localizes with $Rab5^+$ structures. Rather than trafficking via $Rab4^+$ and $Rab11^+$ endosomal compartments, FcεRI appears to ultimately traffic through the $Rab7^+$ late endosomes and LAMP-1^+ lysosomes in a time-dependent manner. The FcεRIα and γ chains remain associated during trafficking. In Syk-deficient cells, the rate of FcεRI migration to lysosomes is markedly enhanced, suggesting that Syk may play a role in modulating receptor traffic.

2. Materials and methods

2.1 Reagents and cell lines

Antibodies and reagents used in this study were obtained from the following vendors: streptavidin AlexaFluor 405, goat-anti-mouse IgG conjugated to AlexaFluor 594, goat-anti-rabbit IgG conjugated to AlexaFluor 647 or AlexaFluor 594, AlexaFluor labeling kits, and cell culture reagents were from Invitrogen Inc. (Carlsbad, CA); anti-DNP-specific mouse IgE clone SPE-7 mAb, dinitrophenyl-conjugated human serum albumin (DNP-HSA), biotinamidohexanoic acid N-hydroxysuccinimide were from Sigma (St. Louis, MO); rabbit polyclonal anti-FcR γ subunit antisera was purchased from Upstate Biotechnology (Lake

Placid, NY); FITC-labeled rat anti-mouse IgE monoclonal antibody (mAb) and purified anti-EEA1 mAb were purchased from BD Biosciences (San Jose, CA); the LAMP-1 mAb used for confocal microscopy originated from J.T. August and J.E.K. Hildreth and was from the Developmental Studies Hybridoma Bank maintained by the University of Iowa, Department of Biological Sciences, Iowa City, IA, USA. Biotinylation of IgE was carried out as described (Cole et al., 1987). AlexaFluor 488 conjugates of anti-DNP IgE were prepared according to the manufacturer's recommendations (Invitrogen Inc.). The wild type EGFP-tagged Rab5 constructs were a kind gift from Dr. Juan Bonifacino (NICHD/NIH, Bethesda, MD). GFP constructs of Rab4, -7, and -11 were kind gifts from Dr. Marino Zerial, Max Plank Institute of Molecular and Cell Biology, Dresden, Germany.

The parental rat basophilic leukemia RBL-2H3 cell line and Syk-deficient RBL-2H3 cells, kindly provided by Dr. Reuben Siraganian (NIDCR/NIH), were cultured as monolayers in ISCOVE's medium (Invitrogen) supplemented with 10% fetal bovine serum, 2 mM glutamine, 0.1 mM non-essential amino acids (all from Biosource International, Camarillo, CA), and 5 μg/ml plasmocin (InvivoGen, San Diego, CA).

2.2 Analysis of surface expression and internalization by flow cytometry

Analyses of FcεRI cell surface expression and receptor internalization were performed as described (Saitoh et al., 2003); (Fattakhova et al., 2006). Adherent RBL-2H3 cells were incubated with 300 ng/ml anti-DNP mouse IgE mAb for 18 h at 37 °C in culture medium. The cells were harvested, and the unbound IgE was washed away, followed by resuspension in Tyrode buffer (10 mM HEPES pH 7.4, 130 mM NaCl, 2.7 mM KCl, 0.4 mM Na_2HPO_4, 1.8 mM $CaCl_2$, 1.3 mM $MgSO_4$, 5.6 mM glucose) at 4×10^5 cells/ml. FcεRI was cross-linked by adding 250 ng/ml DNP-HSA for the indicated lengths of time. Internalization was stopped by placing cells at 4 °C and washing with ice-cold PBS. Cells were blocked with 5% rat serum for 30 min at 4 °C on ice to prevent non-specific staining with secondary Ab and then incubated with FITC-labeled rat anti-mouse IgE for 30 min on ice. For the analysis of total (surface plus intracellular) IgE, cells were fixed with 2.5% paraformaldehyde for 20 minutes at room temperature and incubated with FITC-labeled rat anti-mouse IgE in permeabilizing buffer (0.1% saponin, 1 mM KCl, 1 mM $MgSO_4$ in PBS). Inhibition of Syk activity by piceattanol was done as described (Lauvrak et al., 2006; Oliver et al., 1994). Briefly, IgE-sensitized cells ($3–5 \times 10^5$/ml) were incubated in the presence of 50 μg/ml piceattanol added in DMSO (5 μl of a 10 mg/ml stock solution per ml of culture medium) or the same amount of DMSO alone for 1 hour prior to antigen stimulation. Flow cytometry was performed on a FACSORT™, and the data were analyzed with FLOWJO™ (Tree Star, Inc., Ashland, OR, USA) or CELLQUEST™ software (BD Biosciences).

2.3 Immunostaining, confocal microscopy, image acquisition and analysis

RBL-2H3 cells were seeded at 7×10^5 cells/ml on glass cover slips (Thomas Scientific, Swedesboro, NJ) in 24 well plates (Corning Costar, Rochester, NY) and cultured in serum-free medium containing IgE-AlexaFluor 488 for 18 hours. For analysis of Rab4, Rab5, Rab7 or Rab11 co-localization, cells were transfected with the appropriate EGFP-tagged construct, and sensitized with biotinylated IgE) 24 hours after transfection. During sensitization, IgE conjugates stain only surface FcεRIα chains in intact living cells. After 16 hours, the cells were washed 3 times with serum-free medium, 400 μl of colorless OptiMEM cell medium (Invitrogen Inc.) was added to each well, and cells were incubated in the presence of 100 ng/ml of DNP-HSA for the indicated periods of time at 37 °C. Cells were then washed 3 times with ice-cold PBS and blocked with 5% rat serum in PBS for 30 minutes on ice. After extensive washing, cells were fixed with 3.7% paraformaldehyde in PBS for 15 minutes at 37 °C, then permeabilized with 0.1% Triton X-100/PBS. γ chain staining was made in fixed and permeabilized cells, as the rabbit anti-γ antibodies are specific for the cytoplasmic region of

γ subunits (Jouvin et al., 1995; Maurer et al., 1996; Repetto et al., 1996). EEA1 and LAMP-1 were visualized using the appropriate primary and secondary antibodies. All incubations with unlabeled antibodies were done at room temperature for 40 minutes with gentle shaking, then, the cells were washed 3 times with permeabilization buffer and stained with the appropriate AlexaFluor 594 or AlexaFluor 647 conjugated secondary antibodies. Streptavidin-AlexaFluor 405 was used to visualize biotinylated IgE.

All images were collected on a Leica TCS SP2 AOBS microscope (Leica Microsystems, Heidelberg GmbH, Mannheim, Germany) at the Biological Imaging Facility (Research Technologies Branch, NIAID, NIH, Bethesda). The images were acquired using an oil immersion 63X objective, NA 1.32 in sequential mode. The protocol for image acquisitions and a combination of lasers and intensities were set appropriately to avoid cross-talk between dyes. Image analysis was done using a Leica Confocal Software version 2.5, build 1104 (Leica Microsystems), Imaris version 5.7.1 (Bitplane AG) and by Adobe Photoshop version 7.0 (Adobe Systems). Movies were made from 3D animation of representative cells constructed from confocal images collected in Z plane (20–30 per section) and animated at 15 frames/second.

Three dimensional (3D) images of representative cells acquired in Z-axis stacks (0.3μm) were analyzed for co-localization using the co-localization-module of the Imaris 5.0.2., 64-bit version software (Bitplane Scientific Solutions) (Costes et al., 2004) and plotted versus time. Co-localization is described as the presence of two fluorochromes close enough that they cannot be resolved optically. The voxel intensites were set by the automatic thresholding feature of the Imaris software. The Pearson's correlation coefficient of co-localized volumes measures the correlation between the intensities of the two labels in the co-localized voxels and is used to express the extent of co-localization (Costes et al., 2004).

3. Results

3.1 Association of FcεRIα and γ chains and localization to EEA1$^+$ early endosomes

To analyze the endocytic trafficking of the FcεRIα and γ chains, we utilized confocal microscopy. The α chains were visualized by their selective binding to IgE conjugated to AlexaFluor 488 (shown as green spots). The intracellular localization of FcεRI was analyzed from 5 minutes until 1 hour after cross-linking with DNP-HSA. The localization of the FcεRIγ chain was followed by staining permeabilized cells with rabbit anti-FcεRIγ Ab (magenta spots). In quiescent cells (time 0 minute), as expected, all of the detected α chain (green) is found on the cell surface (Fig. 1, Movie 1 in supplementary material). Similarly, much of the γ chain is also localized at the cell membrane, but, as the total cellular γ chains are visualized, significant amounts are also detected intracellularly. By 5 minutes after receptor aggregation, a significant proportion of the α and γ chains co-localized intracellularly (data not shown). By 30–60 minutes of exposure to antigen, the receptor chains reveal co-localization (white spots) indicating their location in the same intracellular transport compartments (Fig. 1, Movie 2 in supplementary material, Fig. S1, panel A, shows non bias quantitative co-localization coefficients). The inability of co-localization to reach 100% reflects the facts that not all of the receptors are internalized (see Fig. 5B) and not all of the γ chains associate with FcεRI (Asai et al., 2000).

At zero minute, essentially no FcεRIα subunit or γ chain localized to the EEA1$^+$ early endosomes (red spots) (Fig. 1). However, by 5 minutes, a significant co-localization of the γ chains with the EEA1$^+$ compartments is observed (data not shown). By 15 minutes, the majority of the α chains and a high percentage of the γ chains co-localize with EEA1$^+$ compartments (yellow or white spots respectively). At 30 minutes after antigen challenge, most of the internalized FcεRIα and -γ chains are associated with EEA1$^+$ compartments (Fig. 1, panel 30

minutes, Movie 3 in supplementary material shows the FcεRIα co-localization). However, as expected, excess free γ chains can always be detected intracellularly at all times (Asai et al., 2000). During more prolonged incubation times, some co-localization of FcεRI chains and EEA1 still can be observed (Fig. 1, panel 60 minutes). (Fig. S2A–D shows additional representative cells for the 0–60 time points respectively; Fig. S2E shows low resolution images for the 0–30 minute time points). The lack of cell surface staining after prolonged incubation of cells with DNP-HSA suggests that FcεRI does not recycle back to membrane during this time period, or that the kinetics of recycling is slow. These data show that, after antigen-induced cross-linking, FcεRI is delivered to early $EEA1^+$ endosomes.

3.2 Minimal localization of FcεRIα and -γ subunits in $Rab4^+$, $Rab5^+$ or $Rab11^+$ endosomes

Rab5 is a major regulator of early endocytic events for multiple classes of receptors (Zerial and McBride, 2001). Therefore, to examine whether internalized FcεRIα and -γ chains are associated with $Rab5^+$ early endosomes, we expressed EGFP-tagged Rab5 (green) in RBL-2H3 cells. Over-expression of Rab5 (Fig. 2) did not affect the rates of internalization or intracellular trafficking of FcεRI (data not shown). Rab5-containing endosomal structures were localized close to nucleus. Although EEA1 and Rab5 markers show significant co-localization, we observed a subset of single-colored structures (either $EEA1^+$ or $Rab5^+$) or domain separation within double-colored compartments (data not shown), in agreement with published data (Lakadamyali et al., 2006). In contrast to our observation of FcεRIα and -γ chains being localized to $EEA1^+$ early endosomes, there was only minimal co-localization of these receptor subunits with $Rab5^+$ structures, first observed at 15 minutes after addition of DNP-HSA (Fig. 2; Fig. S3 shows enlargements of the panels depicting the merged fluorescent stainings; Fig. S4 A and B shows additional representative cells for the 30 and 60 minute time points respectively; Fig. S1, panel B, shows a plot of the non-bias, quantitative co-localization coefficients versus time).

We next investigated whether ligated FcεRI co-localized with endocytic compartments marked by Rab4 and Rab11. We observed no significant co-localization of the FcεRIα or -γ chains with Rab4 (Fig 3A; Fig. S1, panel C; Fig. S5 A and B show images for additional representative cells for the 60 and 120 minute time points respectively) or Rab11 (Fig. 3B; Fig. S1, panel D; Fig. S6 shows images for additional representative cells for the 60 minute time point) at any time point following receptor ligation. Taken together, these results suggest that aggregated FcεRI does not recycle back to the cell surface, at least in the time period examined.

3.3 Trafficking of aggregated FcεRI to $Rab7^+$ late endosomes and LAMP-1^+ compartments

As discussed above, endocytic processing often involves trafficking from early to late endosomes and eventually to lysosomes. We therefore examined the time-dependent trafficking of FcεRIα and γ chains to these compartments upon receptor aggregation. Using EGFP-tagged Rab7 to visualize late endosomes, we observed a number of large $Rab7^+$ vesicular structures distributed in the cytoplasm of quiescent RBL-2H3 cells (Fig. 4). The IgE-complexed FcεRIα and -γ chains start to accumulate in $Rab7^+$ late endosomes by 30 minutes after FcεRI ligation (Fig. 4, Movie 4 in supplementary material, with maximal accumulation being observed at 2 hours (Fig. 4; Movie 5 in supplementary material; Fig S7 A and B, show images for additional representative cells for the 60 and 120 minute time points respectively; Fig S1, panel E, shows a plot of the non-bias quantitative co-localization coefficients versus time). Staining with LAMP-1 Ab revealed diffuse staining throughout the cells with greater concentrations in regions close to plasma membrane (Fig. 5A). This is consistent with the fact that LAMP-1, as well as the other lysosome-associated membrane proteins, continuously shuttles between the lysosome and the plasma membrane (Eskelinen et al., 2003;Furuno et al., 1989;Lippincott-Schwartz and Fambrough, 1987). Confocal images show that significant amounts of anti-IgE-FcεRI complexes are detected in LAMP-1^+ vesicular clusters at 15

minutes after receptor ligation (Fig. 5A, Movie 6 in supplementary material) and co-localization between FcεRIα or -γ chains and LAMP-1 continued to increase until the last time point examined (2 hours) (Fig. 5A, Movie 7 in supplementary material, Fig S1, panel F, shows a plot of the non-bias quantitative co-localization coefficients versus time).

Following FcεRI aggregation, the tyrosine kinase, Syk, is central to the initiation of downstream signaling leading to mast cell activation (Gilfillan and Tkaczyk, 2006). Therefore, we examined whether Syk plays a role in endocytic trafficking. We observed that the kinetics of the decrease in cell surface FcεRIα chain staining following receptor aggregation was the same in the Syk-deficient and the wild type RBL-2H3 cells (Fig. 5B, left panel). Surprisingly, however, there was a marked decrease in the total pool of FcεRI in the Syk-deficient RBL-2H3 cells following receptor aggregation when compared to wild type cells, suggesting a higher rate of degradation of the receptor in the absence of Syk. We then examined FcεRI endocytic processing in Syk-deficient RBL-2H3 cells by confocal microscopy. The co-staining of FcεRIα and -γ with the early endosomal marker EEA1 revealed no differences between $Syk^{-/-}$ and wild type RBL-2H3 cells (data not shown). In contrast, however, the rate of receptor accumulation in lysosomes was markedly increased in $Syk^{-/-}$ RBL-2H3 cells compared to wild type cells. In $Syk^{-/-}$ RBL-2H3 cells, LAMP-1^{+} vesicles containing both FcεRIα and -γ chains start to appear as early as 5 minutes after FcεRI ligation. After 30 minutes of antigen challenge, a significant portion of the FcεRI complexes are found in LAMP-1^{+} structures and after 60 minutes of cell activation, almost all of the complexes were detected there (Fig. 5C, Fig S8, shows additional representative cells for co-localization of LAMP-1 with FcεRIα or -γ chains in $Syk^{+/+}$ and $Syk^{-/-}$ cells for the 30 minute time point). This faster ingress of FcεRI into the lysosomes in $Syk^{-/-}$ RBL-2H3 compared to wild type RBL-2H3 cells is illustrated by plotting the extent of FcεRIα with LAMP-1 co-localization over time (Fig. 5D). The faster trafficking of FcεRI to lysosomes explains the decreased total amount detected by flow cytometry (Fig. 5B, left panel).

We next determined if FcεRI trafficking was directly related to Syk kinase activity by using piceatannol to inhibit Syk (Oliver et al., 1994). We examined the expression of both surface and total IgE-bound receptors by flow cytometry with an anti-IgE mAb in RBL-2H3 cells treated with 50 μg/ml of piceatannol or solvent only. Figure 5B (right panel) shows that the kinetics of FcεRI internalization was the same in piceatannol-treated versus cells treated with solvent only except for the earliest time point examined (71% of surface expression at 1 minute in non-treated vs. 83% in treated cell. The total FcεRI did not show significant differences at any time point in cells treated with piceatannol versus those treated with solvent only. As a control, we observed that piceatannol treatment significantly blocked β-hexosaminidase release (data not shown), demonstrating that Syk kinase mediated responses in the RBL-2H3 cells were inhibited. From these data, we conclude that the ability of Syk to modify the rate of FcεRI degradation was independent of its catalytic activity.

4. Discussion

Our previous study (Fattakhova et al., 2006) focused on the early membrane-associated events related to the internalization of the FcεRI following aggregation. In this study, we have now investigated the subsequent intracellular trafficking and compartmentalization of the aggregated receptor following internalization with the use of confocal microscopy. The data presented is consistent with the conclusion that FcεRI is internalized into the EEA1^{+} early endosomal compartments (Fig. 1) and that some FcεRI can be detected in Rab5^{+} compartments (Fig. 2), but not the Rab4^{+} or Rab11^{+} endosomal compartments (Fig. 3). Ultimately, it appears in Rab7^{+} (Fig. 4) and LAMP-1^{+} compartments (Fig 5A). Furthermore, we provide evidence that Syk may be required to prolong the half life of the receptor complex once internalized (Fig 5B, & -D), perhaps through its physical association with FcεRI.

Our demonstration that IgE-FcεRIα and -γ chains appear in EEA1$^+$ early endosomes within 15 minutes of aggregation with antigen, reaching maximal accumulation at 30 minutes (Fig. 1), contrasts somewhat with a report (Molfetta et al., 2005) in which FcεRI receptors were observed in transferrin-positive endosomes after 40–60 minutes of incubation with anti-FcεRIα chain mAb. [Transferrin, through its binding to transferrin receptor, is a well-studied marker used to identify early and recycling endosomes (Oksvold et al., 2002)]. It is possible that different modes of aggregation account for this difference i.e. antibody versus IgE-antigen complexes. Regardless, we propose that aggregated FcεRI and transferrin receptor are initially endocytosed into distinct early endosomal compartments, possibly because transferrin receptor endocytosis is clathrin-mediated (van Dam and Stoorvogel, 2002), whereas our data indicates that IgE aggregated FcεRI endocytosis is clathrin-independent and lipid raft-mediated (Fattakhova et al., 2006). Even if endocytosis of aggregated FcεRI is under certain conditions, such as low ligand concentrations (Polo and Di Fiore, 2006), clathrin-mediated as others have reported (Xue et al., 2007), it would not be surprising to find them localized to early endosomal compartments distinct from where transferrin receptors localize (Lakadamyali et al., 2006). The fact that we see only minimal colocalization with Rab5 in the early endosomal compartments is consistent with the observation that Rab22a regulates the recycling of membrane proteins internalized independently of clathrin (Weigert et al., 2004).

While endocytosis from the plasma membrane can occur by a variety of mechanisms, all routes appear to lead to the early endosomal compartment (Mayor and Pagano, 2007). Molecules that have been internalized are then either routed toward lysosomes for degradation or are reutilized by recycling. There is evidence supporting the existence of different regions or subdomains within early endosomes, such that different receptors may remain segregated within this common compartment (Gruenberg, 2001). The compartments within early endosomes that are marked by Rab5 and EEA1 are not entirely overlapping (de Toledo et al., 2003; Galperin and Sorkin, 2003; Lakadamyali et al., 2006). This likely explains why we observe abundant co-localization of aggregated FcεRI with EEA1 (Fig. 1), but much less with Rab5 (Fig. 2). Indeed, a recent study of another immune system activating receptor, KIR2DL4, also showed a disproportionate co-localization, albeit with the opposite pattern of co-localization (Rajagopalan et al., 2006).

From the early endosomes, activation receptors that need to be down-regulated following the initiation of specific cell responses, such as the TCR (Liu et al., 2000) and BCR (Cheng et al., 1999) are shuttled to late endosomes prior to lysosomes for degradation (van der Goot and Gruenberg, 2006). In a similar fashion, our data show that at later times (120 minutes) aggregated FcεRI is predominantly localized to the Rab7$^+$-late endosomes (Fig. 4) and LAMP-1$^+$ compartments (Fig. 5A). Our data indicate that at least the FcεRIα and γ subunits remain associated during endocytic processing, which agrees with previous data indicating that the FcεRI tetrameric complex is processed intact (Molfetta et al., 2005; Quarto et al., 1985). The targeting of signaling receptors to late endosomes/lysosomes is thought to serve to attenuate the signaling response and render cells unresponsive until a new complement of receptors is synthesized (Katzmann et al., 2002). We have employed tagged IgE to track aggregated FcεRI complexes. The fact that the binding of IgE to FcεRI is characterized by a high affinity constant (Sterk and Ishizaka, 1982) and that the internalized IgE remains bound to the receptors until complex degradation (Jensen et al., 2003) makes us confident in the reliability of this approach. This is supported by the observation that the internalized IgE is always found co-localized with FcεRIγ

Previous studies have revealed that Syk can regulate the intracellular traffic of endocytosed receptors (Bonnerot et al., 1998; Le Roux et al., 2007). However, in our study, the kinetics of the decrease in cell surface staining in Syk$^{-/-}$ RBL-2H3 cells was the same as in wild type RBL-2H3 cells (Fig. 5B), indicating that FcεRI endocytosis is independent of Syk. This agrees

with the previous observations that the endocytosis of Fc receptor γ chain following receptor aggregation is independent of Syk activity (Bonnerot et al., 1998) and the kinetics of internalization of B cell receptor is unaffected in $Syk^{-/-}$ B cells (Le Roux et al., 2007). In contrast to surface expression, we observed an accelerated decrease in the total aggregated FcεRI present in antigen-activated $Syk^{-/-}$ RBL-2H3 cells. This more rapid decrease in total FcεRI correlated with an increased rate of FcεRI accumulation in the lysosomes (Fig 5D). These observations were somewhat unexpected in light of a previous report that c-Cbl mediates polyubiquitinylation of FcεRI in RBL-2H3 cells, which may control proteosomal targeting and degradation (Paolini and Kinet, 1993), was Syk dependent (Paolini et al., 2002). However, the regulation of receptor endosomal sorting by Syk may not only be a consequence of its tyrosine kinase activity, but could also be dependent on the physical interaction of Syk with FcεRI. Treatment of wild type RBL-2H3 with the selective Syk-kinase inhibitor piceatannol had minimal effects on FcεRI internalization and did not reduce total receptor levels (Fig. 5B, right panel). This led us to tentatively conclude that recruitment and association of Syk with aggregated FcεRI rather than its kinase activity is important for extending the half-life of the FcεRI. In this respect, it is of interest that recent reports suggest that Syk can function as a membrane adaptor molecule independently of its catalytic activity (Abudula et al., 2007; Kulathu et al., 2008). Thus, although the kinase activity may be necessary for proteosomal degradation, the physical association with Syk may serve to slow endosomal processing leading to degradation in the lysosomes. The functional consequence of this may be extension of FcεRI-mediated signaling in the form of endosomal signaling. This is supported by our preliminary observation that the localization of aggregated FcεRI to endosomal compartments correlates with detection of phosphotyrosine residues in these compartments that were not present prior to FcεRI internalization (data not shown).

In summary, our data shows that aggregated FcεRI traffics to early $EEA1^{+}$ endosomes, but not to $Rab4^{+}$ early/sorting or $Rab7^{+}$ recycling endosomes, and eventually to late endosomes and lysosomes. Our data suggests that Syk kinase may play an essential role in traffic regulation and retention of FcεRI in endosomes.

Supplementary Material

Refer to Web version on PubMed Central for supplementary material.

Acknowledgements

We would like to thank Drs. Juraj Kabat and Owen Schwartz for help with confocal microscopy and Drs. Juan Bonifacino and Marino Zerial for providing the reagents and Reuben Siraganian for the cell lines. We thank Giovanna Peruzzi for her critical comments.

This work was supported by funds from the Division of Intramural Research, NIAID/NIH.

References

Abudula A, Grabbe A, Brechmann M, Polaschegg C, Herrmann N, Goldbeck I, Dittmann K, Wienands J. SLP-65 signal transduction requires Src homology 2 domain-mediated membrane anchoring and a kinase-independent adaptor function of Syk. J Biol Chem 2007;282:29059–66. [PubMed: 17681949]

Asai K, Fujimoto K, Harazaki M, Kusunoki T, Korematsu S, Ide C, Ra C, Hosoi S. Distinct aggregation of beta- and gamma-chains of the high-affinity IgE receptor on cross-linking. J Histochem Cytochem 2000;48:1705–16. [PubMed: 11101638]

Bonnerot C, Briken V, Brachet V, Lankar D, Cassard S, Jabri B, Amigorena S. syk protein tyrosine kinase regulates Fc receptor gamma-chain-mediated transport to lysosomes. EMBO J 1998;17:4606–16. [PubMed: 9707420]

Cheng PC, Steele CR, Gu L, Song W, Pierce SK. MHC class II antigen processing in B cells: accelerated intracellular targeting of antigens. J Immunol 1999;162:7171–80. [PubMed: 10358163]

Cole SR, Ashman LK, Ey PL. Biotinylation: an alternative to radioiodination for the identification of cell surface antigens in immunoprecipitates. Mol Immunol 1987;24:699–705. [PubMed: 3309626]

Costes SV, Daelemans D, Cho EH, Dobbin Z, Pavlakis G, Lockett S. Automatic and quantitative measurement of protein-protein colocalization in live cells. Biophys J 2004;86:3993–4003. [PubMed: 15189895]

de Toledo M, Senic-Matuglia F, Salamero J, Uze G, Comunale F, Fort P, Blangy A. The GTP/GDP cycling of rho GTPase TCL is an essential regulator of the early endocytic pathway. Mol Biol Cell 2003;14:4846–56. [PubMed: 12960428]

Eskelinen EL, Tanaka Y, Saftig P. At the acidic edge: emerging functions for lysosomal membrane proteins. Trends Cell Biol 2003;13:137–45. [PubMed: 12628346]

Fattakhova G, Masilamani M, Borrego F, Gilfillan AM, Metcalfe DD, Coligan JE. The high-affinity immunoglobulin-E receptor (FcepsilonRI) is endocytosed by an AP-2/clathrin-independent, dynamin-dependent mechanism. Traffic 2006;7:673–85. [PubMed: 16637889]

Furuno K, Ishikawa T, Akasaki K, Yano S, Tanaka Y, Yamaguchi Y, Tsuji H, Himeno M, Kato K. Morphological localization of a major lysosomal membrane glycoprotein in the endocytic membrane system. J Biochem (Tokyo) 1989;106:708–16. [PubMed: 2691512]

Galperin E, Sorkin A. Visualization of Rab5 activity in living cells by FRET microscopy and influence of plasma-membrane-targeted Rab5 on clathrin-dependent endocytosis. J Cell Sci 2003;116:4799–810. [PubMed: 14600265]

Geisler C. TCR trafficking in resting and stimulated T cells. Crit Rev Immunol 2004;24:67–86. [PubMed: 14995914]

Gilfillan AM, Tkaczyk C. Integrated signalling pathways for mast-cell activation. Nat Rev Immunol 2006;6:218–30. [PubMed: 16470226]

Gruenberg J. The endocytic pathway: a mosaic of domains. Nat Rev Mol Cell Biol 2001;2:721–30. [PubMed: 11584299]

Jensen BM, Hansen JB, Dissing S, Gerwien J, Skov PS, Poulsen LK. Monomeric immunoglobulin E stabilizes FcepsilonRIalpha from the human basophil cell line KU812 by protecting it from natural turnover. Clin Exp Allergy 2003;33:655–62. [PubMed: 12752595]

Jouvin MH, Numerof RP, Kinet JP. Signal transduction through the conserved motifs of the high affinity IgE receptor Fc epsilon RI. Semin Immunol 1995;7:29–35. [PubMed: 7612892]

Kapp-Barnea Y, Ninio-Many L, Hirschberg K, Fukuda M, Jeromin A, Sagi-Eisenberg R. Neuronal calcium sensor-1 and phosphatidylinositol 4-kinase beta stimulate extracellular signal-regulated kinase 1/2 signaling by accelerating recycling through the endocytic recycling compartment. Mol Biol Cell 2006;17:4130–41. [PubMed: 16837555]

Katzmann DJ, Odorizzi G, Emr SD. Receptor downregulation and multivesicular-body sorting. Nat Rev Mol Cell Biol 2002;3:893–905. [PubMed: 12461556]

Kraft S, Kinet JP. New developments in FcepsilonRI regulation, function and inhibition. Nat Rev Immunol 2007;7:365–78. [PubMed: 17438574]

Kulathu Y, Hobeika E, Turchinovich G, Reth M. The kinase Syk as an adaptor controlling sustained calcium signalling and B-cell development. EMBO J 2008;27:1333–44. [PubMed: 18369315]

Lakadamyali M, Rust MJ, Zhuang X. Ligands for clathrin-mediated endocytosis are differentially sorted into distinct populations of early endosomes. Cell 2006;124:997–1009. [PubMed: 16530046]

Lauvrak SU, Walchli S, Iversen TG, Slagsvold HH, Torgersen ML, Spilsberg B, Sandvig K. Shiga toxin regulates its entry in a Syk-dependent manner. Mol Biol Cell 2006;17:1096–109. [PubMed: 16371508]

Le Roux D, Lankar D, Yuseff MI, Vascotto F, Yokozeki T, Faure-Andre G, Mougneau E, Glaichenhaus N, Manoury B, Bonnerot C, Lennon-Dumenil AM. Syk-dependent Actin Dynamics Regulate Endocytic Trafficking and Processing of Antigens Internalized through the B-Cell Receptor. Mol Biol Cell 2007;18:3451–62. [PubMed: 17596518]

Lippincott-Schwartz J, Fambrough DM. Cycling of the integral membrane glycoprotein, LEP100, between plasma membrane and lysosomes: kinetic and morphological analysis. Cell 1987;49:669–77. [PubMed: 3107839]

Liu H, Rhodes M, Wiest DL, Vignali DA. On the dynamics of TCR:CD3 complex cell surface expression and downmodulation. Immunity 2000;13:665–75. [PubMed: 11114379]

Markgraf DF, Peplowska K, Ungermann C. Rab cascades and tethering factors in the endomembrane system. FEBS Lett 2007;581:2125–30. [PubMed: 17316615]

Maurer D, Fiebiger S, Ebner C, Reininger B, Fischer GF, Wichlas S, Jouvin MH, Schmitt-Egenolf M, Kraft D, Kinet JP, Stingl G. Peripheral blood dendritic cells express Fc epsilon RI as a complex composed of Fc epsilon RI alpha- and Fc epsilon RI gamma-chains and can use this receptor for IgE-mediated allergen presentation. J Immunol 1996;157:607–16. [PubMed: 8752908]

Maxfield FR, McGraw TE. Endocytic recycling. Nat Rev Mol Cell Biol 2004;5:121–32. [PubMed: 15040445]

Mayor S, Pagano RE. Pathways of clathrin-independent endocytosis. Nat Rev Mol Cell Biol 2007;8:603–12. [PubMed: 17609668]

Molfetta R, Belleudi F, Peruzzi G, Morrone S, Leone L, Dikic I, Piccoli M, Frati L, Torrisi MR, Santoni A, Paolini R. CIN85 regulates the ligand-dependent endocytosis of the IgE receptor: a new molecular mechanism to dampen mast cell function. J Immunol 2005;175:4208–16. [PubMed: 16177060]

Oksvold MP, Skarpen E, Widerberg J, Huitfeldt HS. Fluorescent histochemical techniques for analysis of intracellular signaling. J Histochem Cytochem 2002;50:289–303. [PubMed: 11850432]

Oliver C, Fujimura A, Silveira ESAM, Orlandini de Castro R, Siraganian RP, Jamur MC. Mast cell-specific gangliosides and FcepsilonRI follow the same endocytic pathway from lipid rafts in RBL-2H3 cells. J Histochem Cytochem 2007;55:315–25. [PubMed: 17164410]

Oliver JM, Burg DL, Wilson BS, McLaughlin JL, Geahlen RL. Inhibition of mast cell Fc epsilon R1-mediated signaling and effector function by the Syk-selective inhibitor, piceatannol. J Biol Chem 1994;269:29697–703. [PubMed: 7961959]

Paolini R, Kinet JP. Cell surface control of the multiubiquitination and deubiquitination of high-affinity immunoglobulin E receptors. EMBO J 1993;12:779–86. [PubMed: 8382611]

Paolini R, Molfetta R, Beitz LO, Zhang J, Scharenberg AM, Piccoli M, Frati L, Siraganian R, Santoni A. Activation of Syk tyrosine kinase is required for c-Cbl-mediated ubiquitination of Fcepsilon RI and Syk in RBL cells. J Biol Chem 2002;277:36940–7. [PubMed: 12145291]

Polo S, Di Fiore PP. Endocytosis conducts the cell signaling orchestra. Cell 2006;124:897–900. [PubMed: 16530038]

Quarto R, Kinet JP, Metzger H. Coordinate synthesis and degradation of the alpha-, beta- and gamma-subunits of the receptor for immunoglobulin E. Mol Immunol 1985;22:1045–51. [PubMed: 2933582]

Rajagopalan S, Bryceson YT, Kuppusamy SP, Geraghty DE, van der Meer A, Joosten I, Long EO. Activation of NK cells by an endocytosed receptor for soluble HLA-G. PLoS Biol 2006;4:e9. [PubMed: 16366734]

Repetto B, Bandara G, Kado-Fong H, Larigan JD, Wiggan GA, Pocius D, Basu M, Gilfillan AM, Kochan JP. Functional contributions of the FcepsilonRIalpha and FepsilonRIgamma subunit domains in FcepsilonRI-mediated signaling in mast cells. J Immunol 1996;156:4876–83. [PubMed: 8648137]

Rivera J, Olivera A. Src family kinases and lipid mediators in control of allergic inflammation. Immunol Rev 2007;217:255–68. [PubMed: 17498064]

Saitoh S, Odom S, Gomez G, Sommers CL, Young HA, Rivera J, Samelson LE. The four distal tyrosines are required for LAT-dependent signaling in FcepsilonRI-mediated mast cell activation. J Exp Med 2003;198:831–43. [PubMed: 12953098]

Sterk AR, Ishizaka T. Binding properties of IgE receptors on normal mouse mast cells. J Immunol 1982;128:838–43. [PubMed: 7054296]

van Dam EM, Stoorvogel W. Dynamin-dependent transferrin receptor recycling by endosome-derived clathrin-coated vesicles. Mol Biol Cell 2002;13:169–82. [PubMed: 11809831]

van der Goot FG, Gruenberg J. Intra-endosomal membrane traffic. Trends Cell Biol 2006;16:514–21. [PubMed: 16949287]

Weigert R, Yeung AC, Li J, Donaldson JG. Rab22a regulates the recycling of membrane proteins internalized independently of clathrin. Mol Biol Cell 2004;15:3758–70. [PubMed: 15181155]

Wilson BS, Steinberg SL, Liederman K, Pfeiffer JR, Surviladze Z, Zhang J, Samelson LE, Yang LH, Kotula PG, Oliver JM. Markers for detergent-resistant lipid rafts occupy distinct and dynamic domains in native membranes. Mol Biol Cell 2004;15:2580–92. [PubMed: 15034144]

Woodman PG. Biogenesis of the sorting endosome: the role of Rab5. Traffic 2000;1:695–701. [PubMed: 11208157]

Xue M, Hsieh G, Raymond-Stintz MA, Pfeiffer J, Roberts D, Steinberg SL, Oliver JM, Prossnitz ER, Lidke DS, Wilson BS. Activated N-formyl peptide receptor and high-affinity IgE receptor occupy common domains for signaling and internalization. Mol Biol Cell 2007;18:1410–20. [PubMed: 17267694]

Zerial M, McBride H. Rab proteins as membrane organizers. Nat Rev Mol Cell Biol 2001;2:107–17. [PubMed: 11252952]

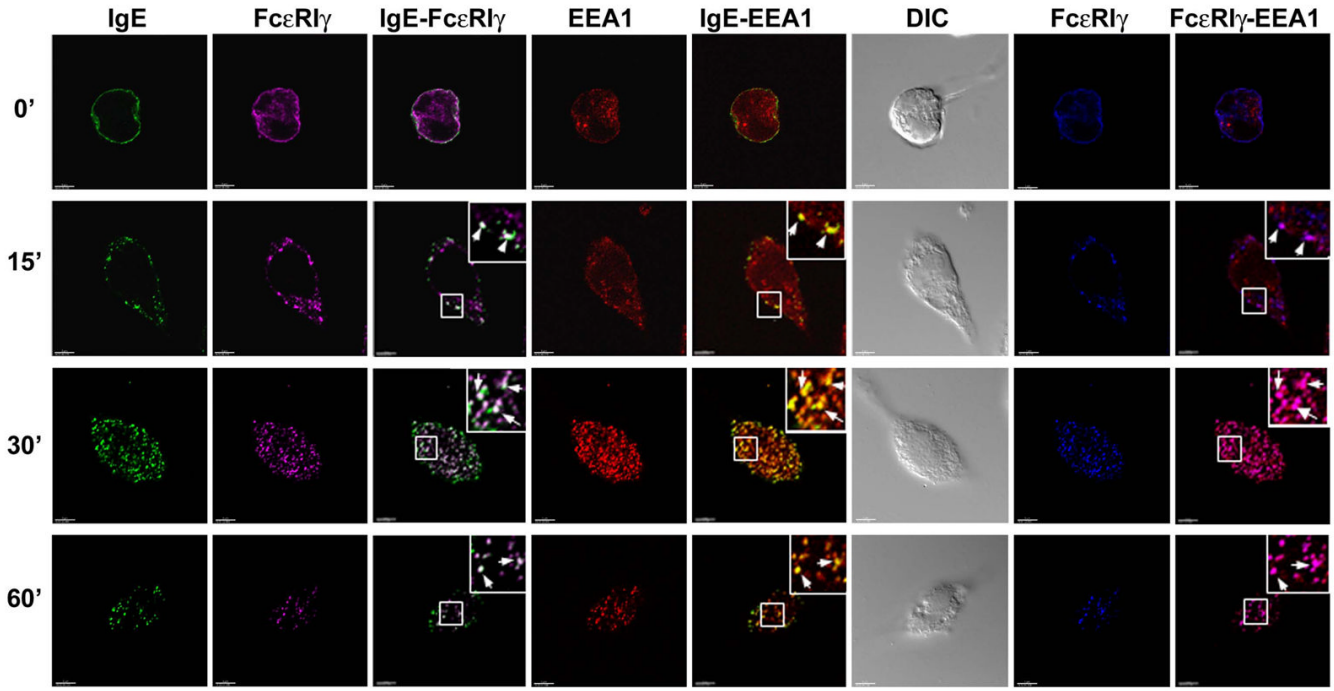

Fig. 1. FcεRIα and -γ chains of cross-linked receptors localize to early endosomes

RBL-2H3 cells were sensitized with anti-DNP IgE-AlexaFluor 488 (shown green) overnight and then incubated with DNP-HSA for the indicated periods of time. Cells were fixed, permeabilized and stained with mouse anti-EEA1 mAb and rabbit anti-FcR γ antibodies. For detection of $EEA1^+$ compartments and FcεRI γ chain, cells were stained with secondary goat-anti-mouse IgG-AlexaFluor 594 (red spots) and goat-anti-rabbit IgG-AlexaFluor 647 (magenta spots) respectively. The cells were then washed, fixed and visualized by confocal microscopy. For analyzing co-localization between FcεRIγ and EEA1, the FcεRIγ is shown in blue (second panels from right). Yellow spots correspond to overlapping between red and green color. The overlap between green and magenta channels results in white spots. The overlap between blue and red channels results in magenta. Squares show areas of cells shown in higher magnification in upper right corner of selected panels. Arrows indicate subcellular structures with co-localization of fluorescent labels. At least 10–20 cells at each time point from three independent experiments were imaged. DIC images are shown in grayscale for all selected cells. Scale bar, 5μm.

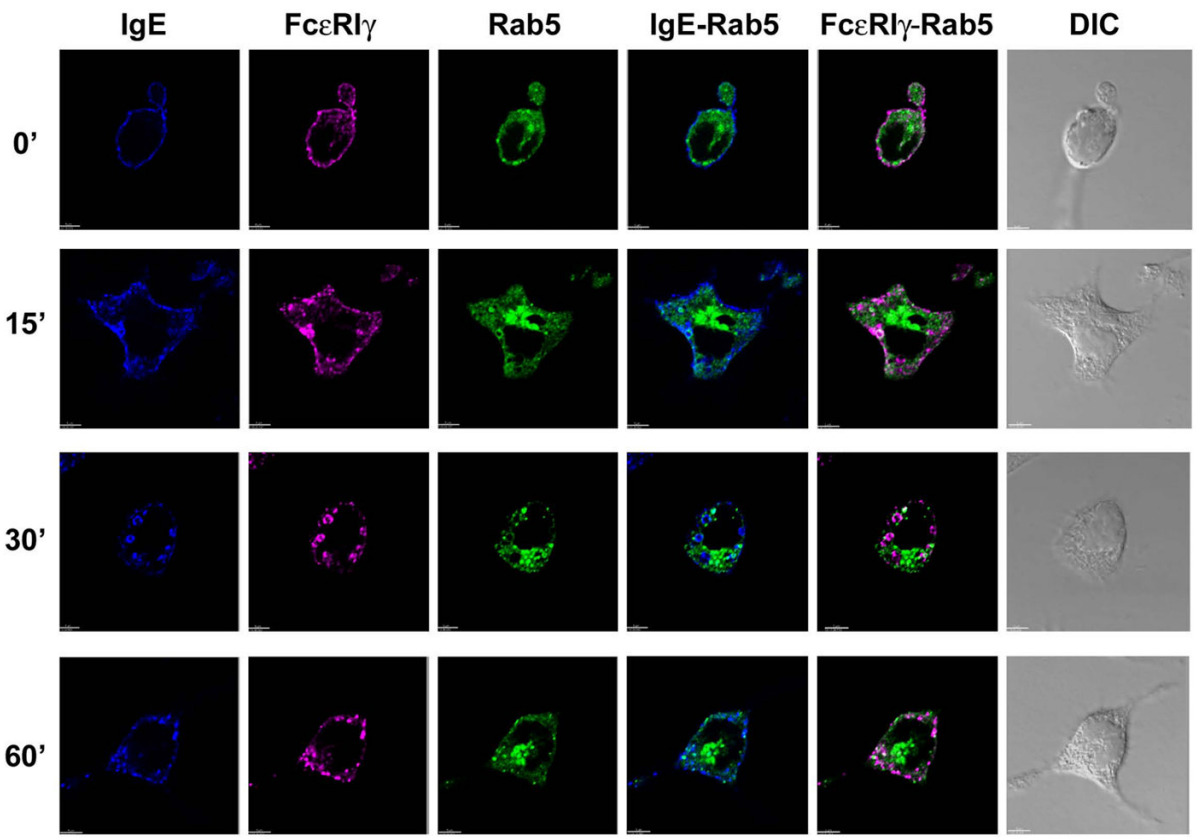

Fig. 2. Endosomal localization of FcεRIα and -γ chains in RBL-2H3 cells over-expressing EGFP-tagged Rab5

RBL-2H3 cells were transfected with EGFP-tagged Rab5 (green), stimulated, stained for IgE with streptavidin AlexaFluor 405 (blue) and for FcεR1γ with rabbit anti-FcR γ antibodies followed by secondary goat-anti-rabbit IgG-AlexaFluor 647 tagged antibody (magenta), and visualized by confocal microscopy following addition of DNP-HSA as described in Materials and Methods. At least 10–20 cells at each time point from three independent experiments were imaged. DIC images are shown in grayscale for all selected cells. The overlap between green and magenta channels results in white spots and the overlap between the green and blue channels results in cyan spots. Scale bar, 5 μm.

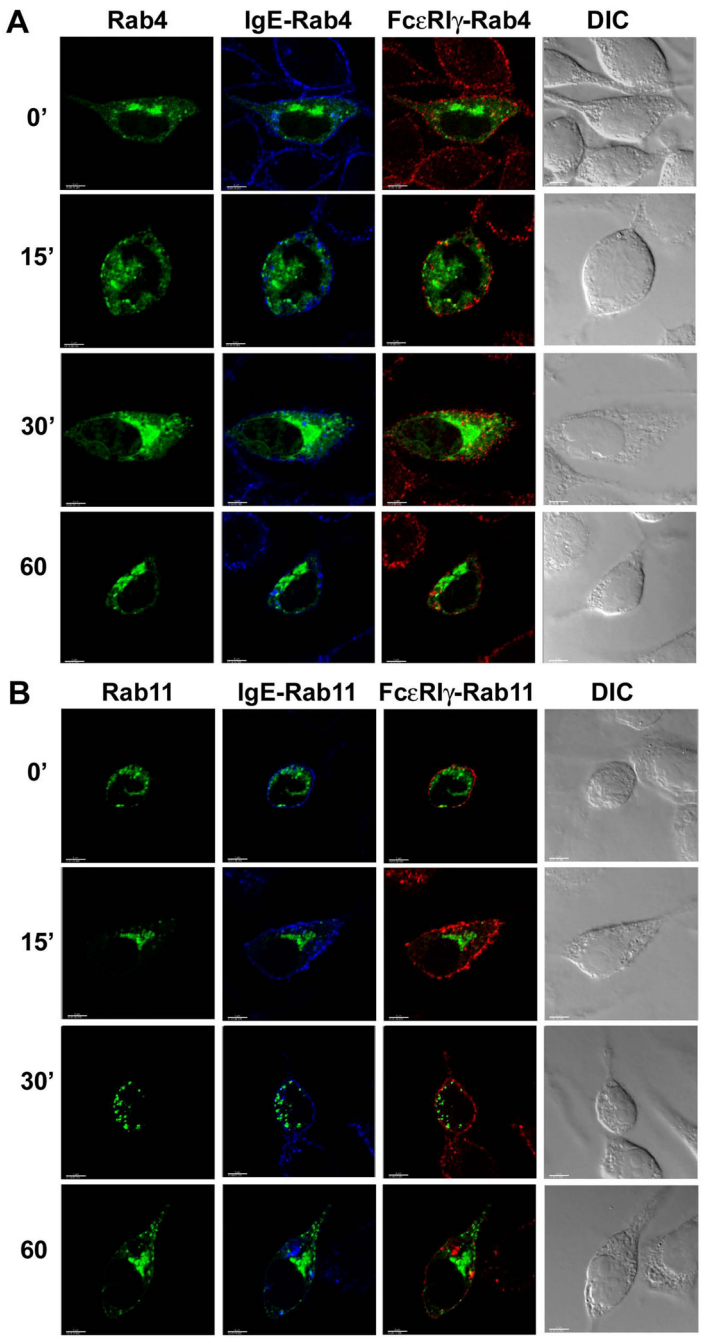

Fig. 3. Localization of FcεRIα and -γ chains in RBL-2H3 cells over-expressing EGFP-tagged Rab4 or EGFP-tagged Rab11

RBL-2H3 cells were transfected with (A) EGFP-tagged Rab4 (green) or (B) EGFP-tagged Rab11 (green), stimulated with DNP-HSA, stained and visualized by confocal microscopy as described in Materials and Methods. IgE-bound FcεRIα chain was detected with streptavidin AlexaFluor 405 (blue) and γ chain was detected with a combination of anti FcR γ antibody and secondary goat-anti-rabbit IgG-AlexaFluor 594 (red) tagged antibody. IgE (FcεRIα) and FcεRIγ stainings are shown merged with the Rab4 or Rab11 images. Yellow spots would indicate co-localization of the red and green colors and cyan staining would indicate co-localization of the green and blue colors. At least 10–20 cells at each time point from three

independent experiments were imaged. DIC images are shown in grayscale for all selected cells. Scale bar, 5μm.

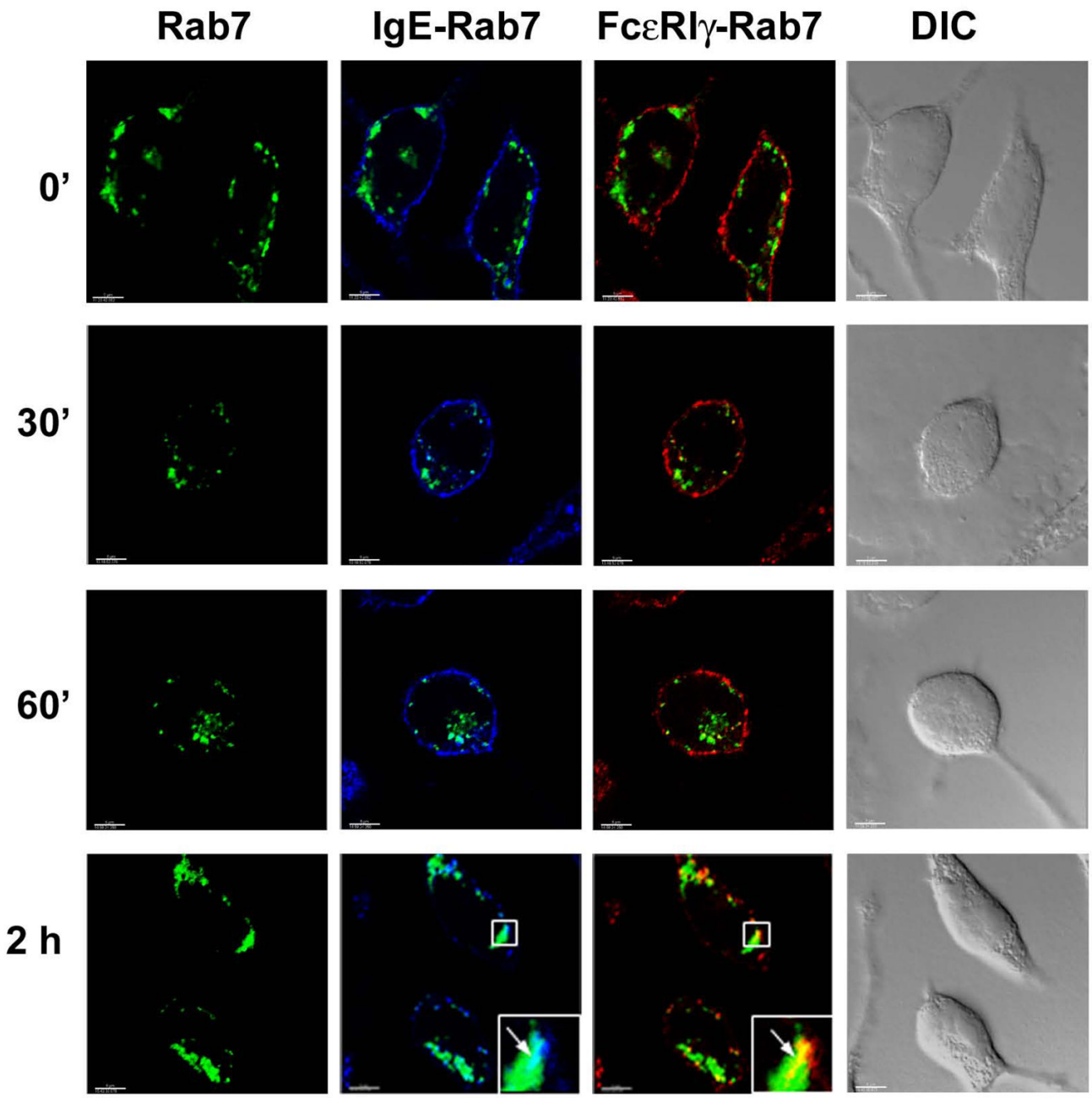

Fig. 4. Localization of FcεRIα and -γ chains in RBL-2H3 cells over-expressing EGFP-tagged Rab7

RBL-2H3 cells were transfected with EGFP-tagged Rab7 (green), stimulated, stained and visualized by confocal microscopy as described in Materials and Methods. IgE-bound FcεRIα chain was detected with streptavidin AlexaFluor 405 (blue), FcεRIγ was detected with a combination of anti FcR γ chain Ab and secondary goat-anti-rabbit IgG-AlexaFluor 594 (red) tagged antibody. IgE-bound FcεRIα and FcεRIγ chains are shown as merged images with EGFP-tagged Rab7. Squares show areas of cells shown in higher magnification in the lower right corner of selected panels. Arrows indicate subcellular structures with co-localization of fluorescent labels. Yellow spots indicate co-localization of the red and green colors and cyan staining indicates co-localization of the green and blue colors. At least 10–20 cells at each time

point from three independent experiments were imaged. DIC images are shown in grayscale. Scale bar, 5μm.

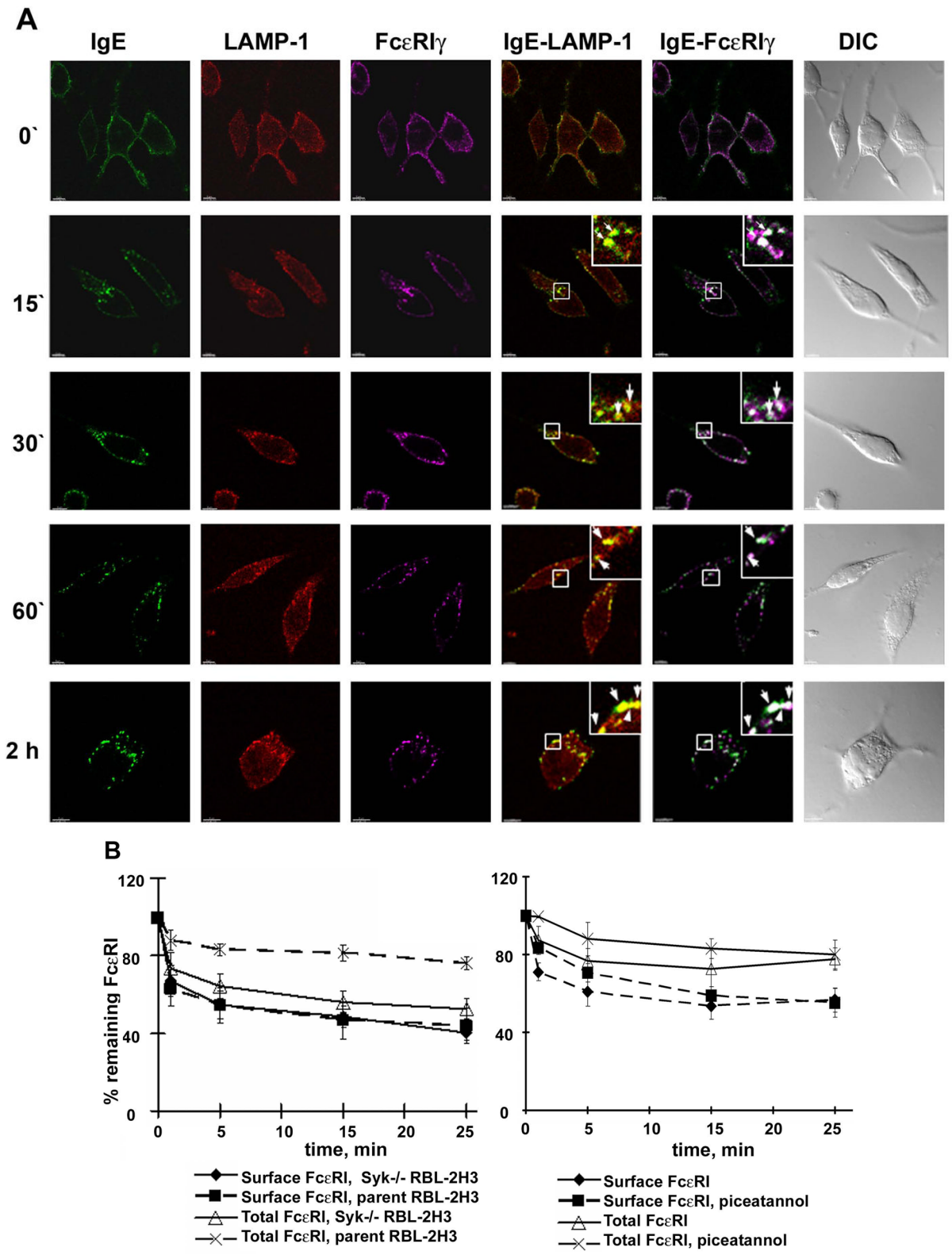

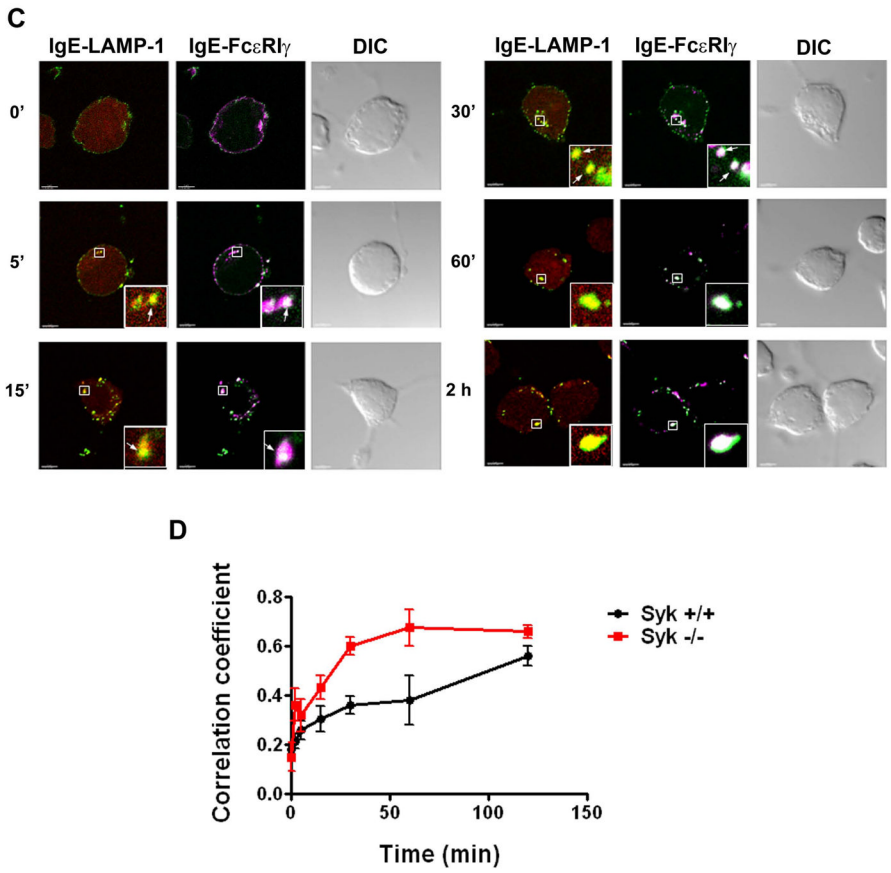

Fig. 5. Ligated FcεRIα and -γ chains traffic to lysosomes is faster in Syk deficient RBL-2H3 cells

A. RBL-2H3 cells were sensitized with IgE-AlexaFluor 488 (shown green) overnight and then incubated with DNP-HSA for the indicated periods of time. Cells were fixed, permeabilized and stained with anti-LAMP-1 mAb and rabbit anti-FcR γ polyclonal Ab. The appropriate secondary Ab were used to visualize lysosomes (red) and FcεRIγ (magenta) respectively. Squares show areas of cells shown in higher magnification in upper right corner of selected panels. Arrows indicate subcellular structures with co-localization of fluorescent labels. Yellow spots indicate co-localization of the red and green colors and white spots indicate co-localization of the green and magenta colors. At least 10–20 cells at each time point from three independent experiments were imaged. DIC images are shown in grayscale. Scale bar, 5μm.

B. Flow cytometric analyses of FcεRI surface and total expression were performed as described in Materials and Methods for RBL-2H3 and Syk$^{-/-}$ RBL-2H3 cells (left panel), and for RBL-2H3 cells pretreated with 50 μg/ml of piceatannol for 1 hour at 37°C (right panel).

C. Syk$^{-/-}$ RBL-2H3 cells were sensitized with IgE-AlexaFluor 488 overnight and then incubated with DNP-HSA for the indicated periods. Anti-LAMP-1 monoclonal antibody and anti-FcR γ polyclonal antibody detected with the appropriate secondary antibody were used to visualize lysosomes (red) and FcεRIγ (magenta) respectively. Merged images of IgE-LAMP-1 and IgE-FcεRIγ are shown. Squares show areas of cells shown in higher magnification in lower right corner of selected panels. Arrows indicate subcellular structures with co-localization of fluorescent labels. Yellow spots indicate co-localization of the red and green colors and white spots indicate co-localization of the green and magenta colors. At least 10–20 cells at each time point from three independent experiments were imaged. Scale bar, 5μm.

D. Co-localization analyses of confocal images for LAMP-1 and FcεRIα (IgE) were performed for the indicated times for wild type (Fig. 5A) and Syk$^{-/-}$ RBL-2H3 (Fig. 5C) cells. The

Pearson's coefficients of co-localized volumes were measured for whole Z- stacks of confocal images using Imaris software and plotted versus time. The data shown are obtained from at least 3–5 confocal stacks of individual cells, representative of three independent experiments. The error bars indicate the standard error of the mean.